CHANGE IN MODAL PARAMETERS OF CRACKED SINGLE-EDGE NOTCHED PLAIN CONCRETE BEAMS *

Luis A. Padrón[1], Juan J. Aznárez[1], Héctor Cifuentes[2],
Fernando Medina[2], Orlando Maeso[1]

[1]University Institute SIANI, Universidad de Las Palmas de G.C., Las Palmas de G.C., Spain
{lpadron,jjaznarez,omaeso}@siani.es

[2]Universidad de Sevilla, Seville, Spain
{bulte,medinaencina}@us.es

September 17, 2015

Abstract

The aim of this work is looking into the possibility of capturing the change in the modal properties (natural frequencies, modal shapes and modal damping ratio) of plain concrete elements due to the presence of cracked areas by using a simple continuum damage zone numerical model. To do so, and as a first step, single-edge plain concrete beams were identified by experimental modal analysis with and without cracks in order to find out how cracking affects the first three flexural modes of the element. Then, numerical modal analysis was performed by finite elements in order to identify the material properties of the intact specimens by model updating and also check the experimental results. Finally, a boundary element – finite element coupled code was used to find a continuum model for the cracked single-edge notched beam able to reproduce the experimental results in terms of natural frequency shifts and modal damping ratios. It was found that, in order to reproduce the experimental frequency response functions, an overdamped damage zone is needed together with an equivalent crack length.

Keywords: Modal analysis, Concrete, Crack Models.

1 INTRODUCTION

There exist mainly two types of approaches to study the behaviour of cracks in concrete structural elements: discrete (i.e. fictitious crack model) or smeared cracking models (i.e. continuum damage models). The first group of models is generally used to predict crack growth and study the behaviour in the immediate vicinity of the damage. However, although being more appealing for being closer to the real situation in plain concrete structures, discrete crack models imply the modelling of individual cracks, which makes it not viable for large real structures with multiple cracks. On the contrary, and specially in cases where the structure is analysed under dynamic loads that do not induce crack growth, and when the points

*Draft of the paper published in JOURNAL OF VIBRATION ENGINEERING & TECHONOLOGIES, 3(3), 253-265 (2015)

of interest are not close to the cracks themselves, linear continuum damage models are a viable alternative if they are capable of reproducing the general influence of the crack on the response of the overall structure. This work focuses in that second situation in which a concrete structural element is already cracked and, not being viable the modelling of every individual crack, it is being submitted to dynamic loads (seismic, for instance, but in any case not large enough to cause crack growth). As already well known [1, 2], the presence of those cracks will modify the structural dynamic response, characterized by its modal parameters (natural frequencies, modal shapes and modal damping ratios), and the estimation of such modification is one of the aims of appropriate crack modelling.

On the other hand, countless works on damage identification can be found in the literature [3], many of which deal with crack location and severity in beams [4, 5, 6, 7, 8, 9, 10, 11, 12, 13, 14]. In this case, modelling the beams as 1D elements and the cracks as rotational springs is a common approach. The focus of the research presented in this work is not on damage identification or 1D modelling, but on cracking modelling in 2D or 3D solids and its influence on the dynamic properties of the system.

In short, the aim of this work is looking into the possibility of capturing the change in the modal parameters by using a simple 2D or 3D continuum damage zone numerical model for cracked concrete elements. To do so, and as a first step, single-edge plain concrete beams are identified by experimental modal analysis with and without damage in order to find out how cracking affects the first three flexural modes of the element. Then, numerical modal analysis is performed by finite elements in order to identify the material properties of the intact specimens by model updating and also check the experimental results. Finally, a boundary element – finite element coupled code is used to find a model of the single-edge notched beam able to reproduce the experimental results obtained from the damaged specimens in terms of natural frequency shifts and modal damping ratios. One of the parameters of such a simplified model is the length of the equivalent notch needed to study the damaged specimen under the linear-elastic hypotheses. The adequate value of this equivalent notch is found to be coincident with the effective crack length given by the two-parameter fracture model for concrete of Jenq and Shah [15]. It is also shown that, besides such equivalent notch length, a high damping ratio in the linking fractured zone is also to reproduce both natural frequency shifts and modal damping ratios.

2 METHODOLOGY

2.1 Overview

This work contains two distinct parts: *a)* an experimental part in which the modal parameters of plain-concrete intact and cracked single-edge notched bending specimens are estimated; and *b)* a numerical part involving different numerical models to address the problem at hand. The details are given in the following sections.

2.2 Specimen description

The test specimens are prismatic single-edge notched bending plain concrete elements of $120 \times 60 \times 570$ mm (height, width, length), with a center notch 3 mm width and 60 mm deep (i.e. 50% of the specimen's height). One specimen is shown in Figures 1 and 2.

Three specimens were produced and tested with a 1/1.7/2.9/0.5 (CEM-I-52.5 cement, sand, crushed rock, water) concrete. The resulting concrete had a density (after 35 days) of $\rho = 2418.8$ kg/m^3. They were dynamically identified (see section 2.3) after approximately

Figure 1: Specimen during a three-point flexural test (left) and detail of cracks after test (right).

35 days. Immediately after identifying the intact specimens, they were subjected to a three-point bending single-edge notched fracture test in order to produce visible cracks with lengths around 30 mm at a first stage (damage state 1), and around 35 mm at a second and final stage (damage state 2), but without reaching total fracture of the element (see Figure 1). Note that those crack lengths given before are only rough estimates of the visible cracks observed at both sides of the specimen, and are not a measure of the fracture process zone, which has not been assessed. The state of the damaged specimen could be understood to be close to that of a beam with a plastic hinge.

2.3 Experimental modal analysis description

The first three natural frequencies, modal shapes and modal damping ratios of the intact and damaged specimens with free-free boundary conditions need to be experimentally identified by experimental modal analysis. The characteristics of the specimen recommend the use of the impact hammer technique [16, 17] to perform the experimental modal analysis. Free-free boundary conditions were used, implemented by hanging the specimen by rubber bands. Since 4 accelerometers were available for the tests, and in order to be able to obtain acceleration records in 7 different positions on the top edge of the specimen, two different setups (see Figure 2) were used in the tests (one accelerometer stays in the same place to work as reference sensor). To be sure that all significant modes were properly excited, the impacts were applied on two different points (A and B in Figure 2). 5 repetitions were recorded for each one of the two setups and two impact points, and for each one of the three specimens in their three states. That would make a total of 180 impact hammer tests, but one of the specimens could not be tested in the second damage state (because of premature failure), so 160 impact test were finally performed.

The technical characteristics of all equipment is detailed in the following: a) Impact hammer: Brüel & Kjaer 8206-001. Reference sensitivity: 11.42 mV/N. Full Scale Force Range Compression: 445 N. Effective seismic mass with enhancement: 140 gr. Aluminum tip; b) Accelerometers: Brüel & Kjaer 4508-002 and 4507-002. Reference sensitivity: 1 V/g.

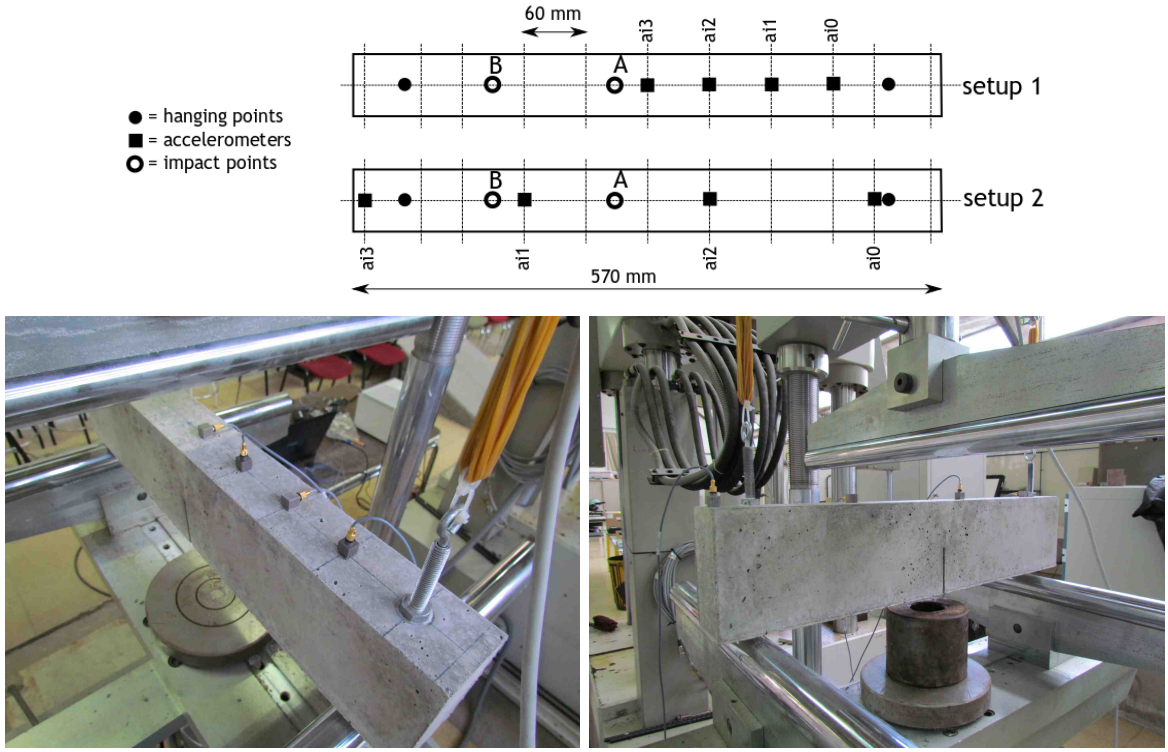

Figure 2: Experimental setups used in the experimental modal analysis by impact hammer. Details of setup 1 (bottom left) and 2 (bottom right).

Frequency: 0.3-8000 Hz. Residual noise level (rms): ±0.35 mg. Mass: 4.8 gr. Beewax is used for mounting; c) DAQ system: NI PXIe-4496, 24-Bit, Sigma-Delta ADCs, on NI PXIe-1073; and d) Acquisition parameters: sampling frequency: 25000 Hz. Pre-trigger at 0.05 N with 100 buffer points.

Figure 3 shows an example of impulse recorded by the impact hammer (left) together with its power spectral density estimation (centre) and a recorded time-history response. The center figure shows that the energy provided to the system can be considered sufficient up to 5000 Hz, while modes above 9000 Hz are not excited at all. The left figure shows that the response damps out completely after around 0.3 s. For this reason, the response is recorded during 0.4 s (10000 samples) and no windowing is necessary.

2.4 Numerical analyses

The calibration of the Young's modulus of the concrete was made by matching the natural frequencies of a numerical model with the experimental natural frequencies. To do so, modal analysis was performed by finite elements using ANSYS® software [18].

Numerical frequency response functions (FRFs), on the other hand, were obtained numerically by a 2D BEM-FEM code in the frequency domain. The concrete specimen has been modeled as an isotropic viscoelastic domain with hysteretic damping model of the type $E = \mathrm{Re}[E](1 + 2\mathrm{i}\xi)$, being ξ the hysteretic damping ratio, and analyzed with the boundary

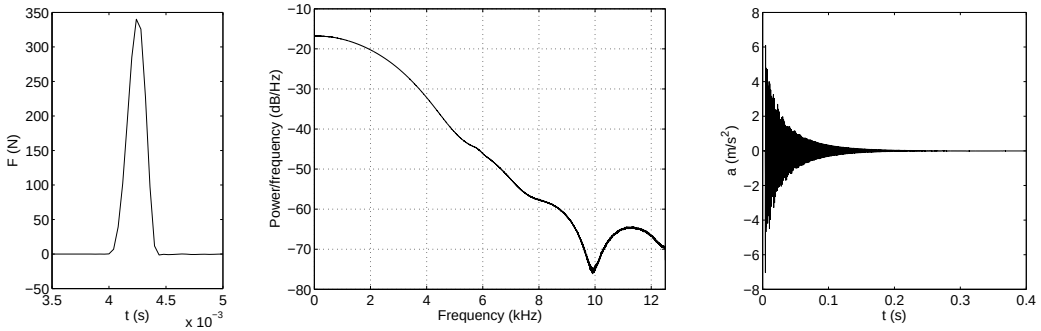

Figure 3: Characterization of the impulse applied for identification. Impulse (left), power spectral density estimation (centre), and recorded time-history response (right).

element method [19] using quadratic elements. The rubber bands are modeled as Euler-Bernoulli beams using 2-node 6-degrees of freedom beam finite elements [20]. The coupling between boundary elements and finite elements is made through plane perfectly rigid surfaces defined by any number of boundary elements, allowing the establishment of equilibrium and compatibility conditions between those boundary elements and the finite element structure attached to them.

2.5 Effective crack length by LEFM assumptions.

Several adaptations of the linear elastic fracture mechanics (LEFM) assumptions have been proposed which take into account the nonlinear fracture behavior in an approximate manner [21]. These adaptations are usually called effective crack models and they take into account the pre-peak nonlinear behavior of concrete and are able to give a good estimate of the peak load. One of the most universal effective crack model is the two parameter model from Jenq and Shah [15]. On the basis of this method, an equivalent elastic structure containing an effective crack whose length is larger than the length of the crack in the real structure should be determined [22]. Then LEFM can be applied to study the fracture behavior of the concrete structure considering the effective crack length. In this way, the damage produced in the fracture process zone ahead the real crack in the concrete structure is considered. The model of Jenq and Shah will be compared here with the results by the BEM-FEM model in terms of modal parameters.

3 RESULTS

3.1 Results from experimental modal analysis.

This subsection summarizes some of the results obtained from the experimental modal analyses performed on the specimens. First of all, and just in order to illustrate the level of repeatability of the experiments, figure 4 presents the moduli of the frequency response functions, relating the response at ai2 to impact point A at setup 1, for the five tests on the intact (left) and most damaged (right) states of the first specimen. In the case of the intact specimen, the identified FRFs are very smooth and virtually independent on the test. As

expected, in the case of the damaged specimen, a small level of non-linearity is observed when the results are analysed in detail. For instance, additional side peaks around resonance (mostly below the second mode and around the first mode) appear when damage exists, which suggests a non-linear behaviour of the cracks in the form of breathing cracks [9]. On the other hand, and only for the most damaged states, for changes of around 60% in the impact level, natural frequencies vary up to a 0.4% and peak magnitudes up to a 30%. For the intact specimens, these non-linearities are virtually nonexistent. It is also worth mentioning that the identified parameters can be considered consistent across repetitions and also across specimens, which suggests that the experimental results are robust. Therefore, and for the sake of clarity, results corresponding only to individual tests on specimen one will be shown in this section.

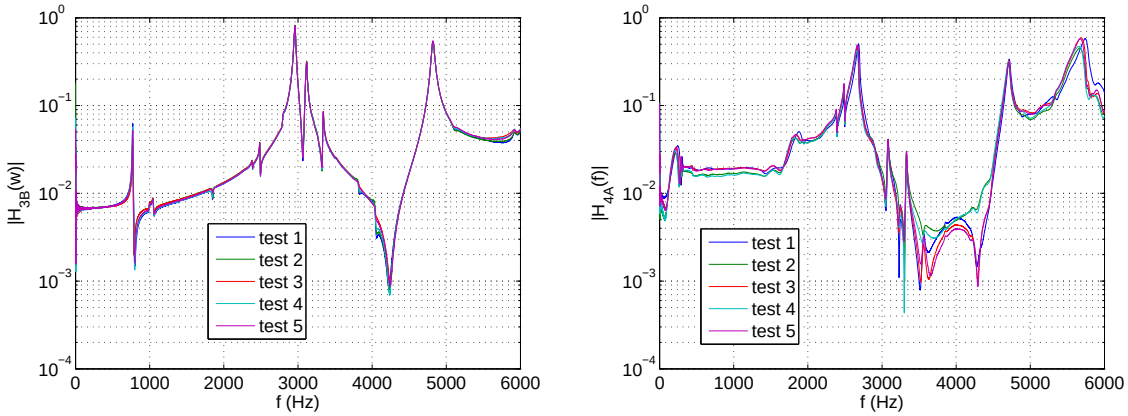

Figure 4: Illustrations of levels of repeatability and non-linearity in the estimated frequency response functions. Setup 1. Measured at 60 mm left from the center (ai2). Impact on point A. Intact specimen (left) and damaged specimen (right).

Table 1 presents the experimentally identified natural frequencies for the intact and damaged states. Figure 5 shows the normalized frequency response functions corresponding to an impact on point A (i.e. 30 mm to the left of the center) and measuring in channel ai2 from setup 1 (i.e. at 60 mm to the right of the center, see Figure 2). Real and imaginary parts are also shown. As expected, frequencies are lower when the element is damaged due to the smaller stiffness of the damaged zone. It can also be seen that, while the fundamental flexural frequency gets reduced by more than 50% from the intact to the first damage state, the second and third frequencies are reduced by only 8 and 2% respectively, showing that, in this specific configuration of the element, the damage affects mainly to the fundamental mode. The difference between the two damage states is much smaller. It is also apparent how the first mode is extremely damped in the damaged specimens, due to the fact that most of the deformation corresponding to that fundamental mode occurs in the central damaged part.

Figure 6 shows the three modal shapes experimentally identified for the different damage states. It is worth mentioning here that the modes do not change significantly between intact or damaged specimens in terms of shapes, although they obviously change in terms of amplitude and frequency. The first mode shape is only shown for the intact state due to the

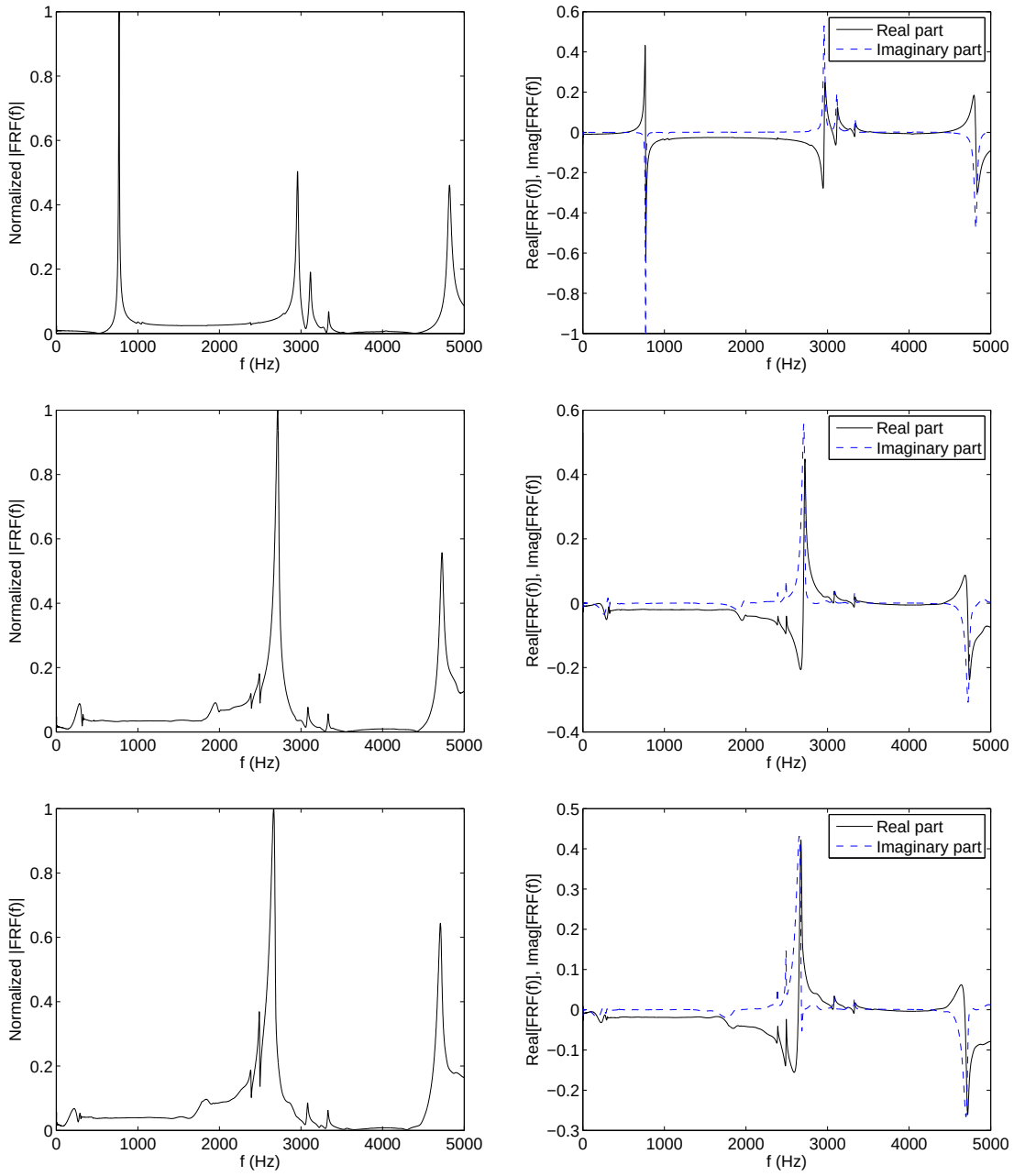

Figure 5: Frequency response functions obtained from experimental modal analysis. Setup 1. Measured at 60 mm left from the center (ai2). Impact on point A. Intact (top), damage state 1 (centre), and damage state 2 (bottom) specimens.

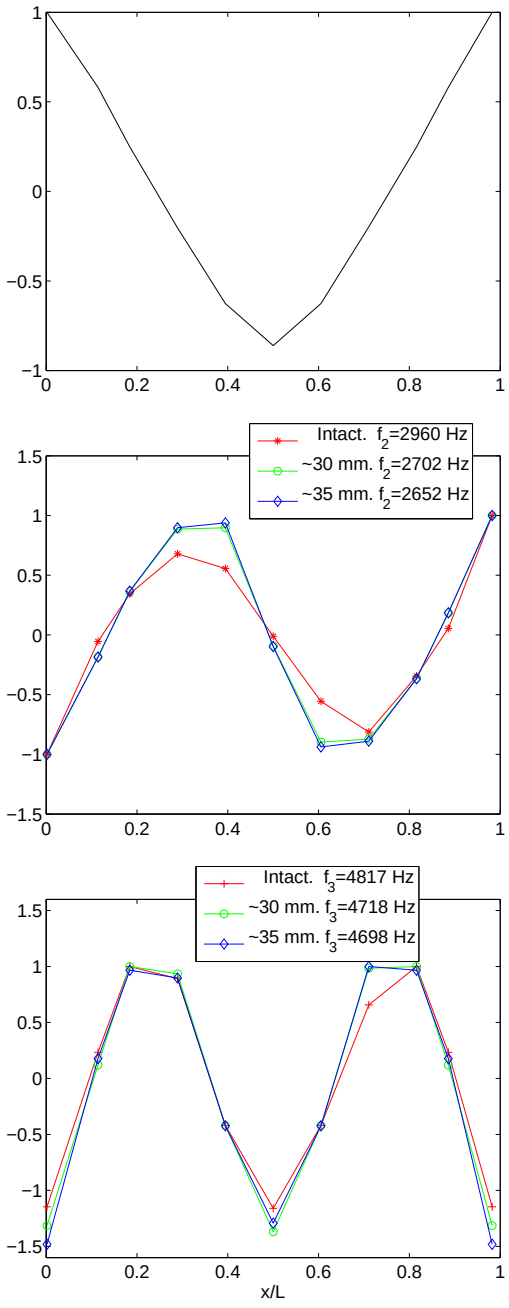

Figure 6: Modal shapes obtained from experimental modal analysis. First (top), second (center) and third (bottom) flexural modes.

	Mode 1	Mode 2	Mode 3
Intact specimen	760	2960	4817
damaged specimen (damage state 1)	∼300	2702	4718
damaged specimen (damage state 2)	∼300	2652	4698

Table 1: Experimentally identified natural frequencies (Hz).

mode overdamping observed for the damaged specimens.

Modal damping ratios were also estimated from the experimental frequency response functions, finding a value of $\xi = 0.005$ (0.5%) for all the three modes of the intact specimen, which supports the use of a frequency-independent hysteretic damping model for the numerical analysis. In the damaged specimen, damping ratios for the second and third modes are slightly larger while the fundamental mode is completely overdamped.

3.2 Results from finite elements modal analysis.

This section presents results from numerical modal analyses performed in order to identify the material Young's modulus by finite–element updating. The geometry of the intact specimen was discretized by 3-D 10-node tetrahedral structural solid elements. Convergence analyses regarding natural frequencies and modal shapes were made in order to define a valid mesh for the analysis. A mesh with 29819 nodes and 19249 elements was found to provide accurate results for the present analysis. The density of the concrete had been previously measured to be $\rho = 2418.8$ kg/m^3. Poisson's ratio was assumed to be $\nu = 0.2$. As only one parameter (material Young's modulus) needed to be identified, and an estimation was already available from static tests on different specimens, a simple 'trial-and-error' approach was used for the model updating. A Young's modulus $E = 3.5 \times 10^{10}$ Pa, very close to the previously available static value for the concrete used for the specimens, was found to match the experimental flexural fundamental frequency. Table 3.2 shows the very good agreement found also for the higher modes. Figure 7 shows the corresponding modal shapes, that agree very well with the experimental ones presented in Figure 6, giving more information about the deformation of the element, not only on the top surface, but as a whole.

Mode	Numerical (Hz)	Experimental (Hz)	Difference (%)
1	760	760	0
2	2917	2960	1.4
3	4651	4817	3.4

Table 2: Comparison between numerical (FEM) and experimental natural frequencies for the intact state.

3.3 Results in the frequency domain from BEM-FEM analysis.

Using the material parameters found in the previous section ($\rho = 2418.8$ kg/m^3, $\nu = 0.2$, $E = 3.5 \times 10^{10}$ Pa, $\xi = 0.005$), the two-dimensional BEM-FEM formulation described above has been used to find a simple damage model for capturing the change in the modal parameters

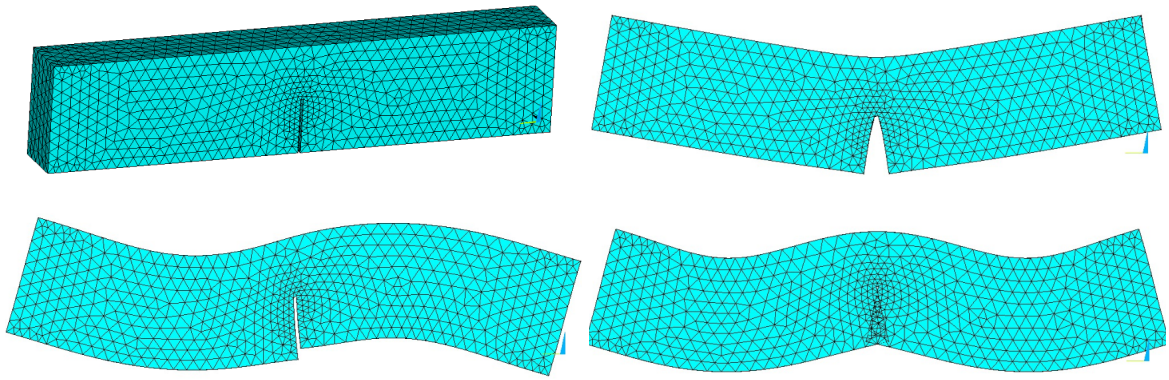

Figure 7: Mesh and first three flexural modal shapes obtained from finite element modal analysis for the intact state.

of the specimen due to the cracks. As shown above, such a model should be able of capturing not only the frequency shifts but also the extremely high damping suffered by the first mode in relationship with the the other modes. The geometry of the intact specimen was discretized by 3-D 10-node tetrahedral structural solid elements. Convergence analyses regarding natural frequencies and modal shapes were made in order to define a valid mesh for the analysis. A mesh with 1196 BEM nodes, 588 BEM 2D quadratic elements, 8 FEM nodes and 6 beam FEM elements was found to provide accurate results for the present analysis.

Experimental results for the intact specimen are very closely reproduced using the original geometry and properties. On the other hand, in the case of the damaged configurations, a model in which a link zone, geometrically modified in order to consider an equivalent crack length larger than the actual crack (see section 2.5 and shadowed area Ω_2 in Figure 8), is given the same density and Young's modulus than the rest of the element but a much higher damping ratio ($\xi_2 = 2.00$) has been found to reproduce very closely the experimental results in terms of both frequency shift and overdamping of the first mode. Equivalent notch lengths of 90 mm and 94 mm are found to provide the best approximations for both modal frequencies and dampings of both damage states.

	Mode 1	**Mode 2**	**Mode 3**
Intact specimen (exp.)	760	2960	4817
Intact specimen (num.)	760	2910	4650
Damage state 1 (exp.)	∼300	2702	4718
90 mm notch & $\xi_2 = 2.0$ (num.)	∼300	2535	4610
Damage state 2 (exp.)	∼300	2652	4698
94 mm notch & $\xi_2 = 2.0$ (num.)	∼300	2473	4606
94 mm notch & $\xi_2 = 0.005$ (num.)	∼300	2578	4646

Table 3: Numerical BEM-FEM natural frequencies vs experimental natural frequencies (Hz).

Table 3 summarizes these results in terms of frequencies, while Figure 9 shows the normal-

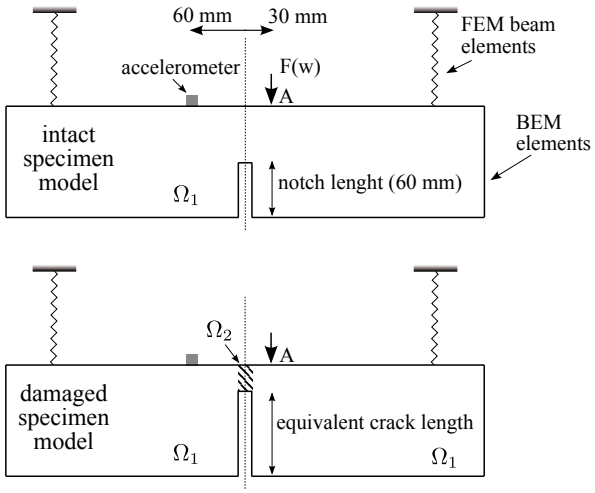

Figure 8: BEM-FEM models for intact (top) and damaged (bottom) specimens.

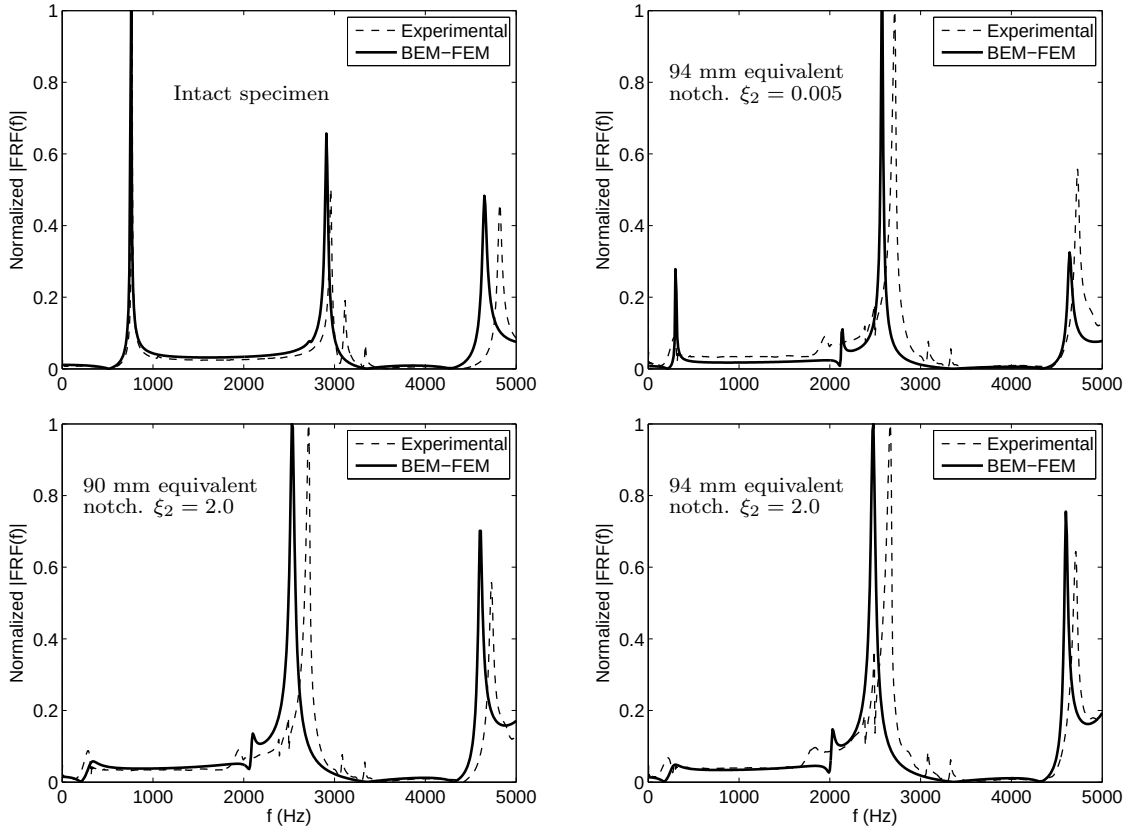

Figure 9: Numerical normalized frequency response functions for different models by BEM-FEM formulation. Measured at 60 mm left from the center (ai2). Impact on point A. Comparison with experimental results from intact (top left), damage state 1 (top right and bottom left) and damage state 2 (bottom right).

ized frequency response functions for most of the described cases. The comparison between these numerical results against the experimental results discussed above, shows the good agreement between this simple model and the experiments. The match is not perfect, but the general trends are indeed captured. Moreover, last row of the table 3 and top right plot of Figure 9 show that the largest equivalent notch length and no additional damping provides the best estimation for the second and third natural frequencies. Such a model, however, is not able to capture properly the overdamping of the first mode due to the damage, or the relationship between the relative peak values of the different modes.

3.4 Equivalent elastic crack length according to Jenq and Shah

Critical effective crack length a_e according to LEFM was obtained with P-CMOD curves in order to compare it with the results of the previous sections and see if these equivalent linear approximations could be used in the future for more complex cases. This was calculated using the compliance method of Jenq and Shah [15]. According to these indications, after obtaining the initial compliance C_i of the P-CMOD curves, the elastic modulus of concrete is obtained as $E_c = 6Sa_oV_1(\alpha')/(C_iBD^2)$, where $V_1(\alpha')$ is a geometric function given by

$$V_1(\alpha') = 0.8 - 1.7\alpha' + 2.4\alpha'^2 + \frac{0.66}{(1-\alpha')^2} + \frac{4D}{S}(-0.04 - 0.58\alpha' + 1.47\alpha'^2 - 2.04\alpha'^3), \quad (1)$$

B is the specimen width, D is the depth of the cross section of the specimen, S is the specimen loading span, L is the specimen length, a_0 is the initial relative notch depth and $\alpha' = (a_0 + HO)/(D + HO)$, in which HO is the clip gauge holder thickness (Figure 10). In this case, HO was 1 mm and there was no accuracy loss if $\alpha' \approx \alpha$ was considered (being $\alpha = a_0/D$ the relative notch depth). The value obtained for $V_1(\alpha)$ was 2.972 and the elastic modulus of concrete was determined.

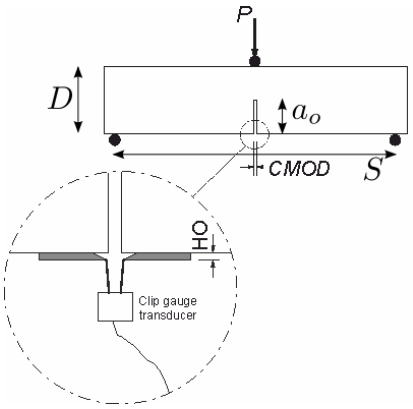

Figure 10: Details of the CMOD instrumentation for the three-point bending tests

Now, the critical effective crack length (a_e) is calculated from E_c and the unloading compliance C_u, which was measured at 95% of the maximum load and assuming the unloading path return to the origin. The critical effective crack length is found when the relationship $E_c = 6Sa_eV_1(\alpha'_e)/(C_uBD^2)$ is satisfied. This way, the obtained unloading compliance from three-point bending tests was 6.477×10^{-5} mm/N $\pm 15\%$ and the obtained value of the critical

crack was $a_e = 90\,\text{mm}$, which coincides exactly with the result of the previous sections once damping has been taken into account. It must be noted that this effective crack length considers, by means of a longer crack length, the stresses relaxation and the stiffness reduction produced in the fracture process zone of quasi-brittle materials (like concrete) when linear elastic models are used.

4 CONCLUSIONS

This work presents a simple continuum damage zone numerical model for cracked concrete elements to capture the change in modal parameters due to damage. A very specific case has been investigated: a single-edge notched plain concrete bending specimen, which leads to an specific configuration close to plastic hinge when damaged.

Several specimens were experimentally identified with and without damage. Several numerical analyses were performed and a model comprised by an equivalent crack length and an overdamped zone is proposed. It is shown that such a model is able to capture the main features of the problem, in terms of both modal frequency shifts and modal dampings. To do so, the equivalent crack length proposed by Jenq and Shah [15] (which allows the static analysis of the damaged specimen under the linear-elastic hypotheses) can be used. In addition to this, in order to be able to reproduce the dynamic response of the system, overdamping must be assigned to the rest of the damaged zone. In any case, in order to be able to draw general conclusions, future developments should involve different and more general configurations and sizes, more damage levels and different concrete mixes.

Acknowledgements

This work was supported by Subdirección General de Proyectos de Investigación of the Ministerio de Economía y Competitividad (MINECO) of Spain through the research project BIA2010-21399-C02-01/02 (coordinated between the Universidad de Las Palmas de Gran Canaria and the Universidad de Sevilla) and co-financed by the European Fund of Regional Development (FEDER). The authors would also like to thank Jacob Montesdeoca for his help in the preparation of specimens and tests; and Rubén Darias, Jacob Rodríguez, Ariel Santana and Ayoze Méndez for their help during the experiments. The three-point flexural tests were performed in the Laboratorio de Construcción of the Escuela de Arquitectura of the Universidad de Las Palmas de Gran Canaria. The specimens and auxiliary equipment were made in the Laboratorio de Hormigones, Tierras y Asfaltos of the EIIC of the same university.

References

[1] P. Cawley and R.D. Adams, Location of defects in structures from measurements of natural frequencies. *J Strain Anal Eng Des*, **14**(2), 49–57, 1979.

[2] P. Gudmundson, Eigenfrequency changes of structures due to cracks, notches or other geometrical changes. *Journal of the Mechanics and Physics of Solids*, **30**(5), 339–353, 1982.

[3] Q.W. Yang, Review of vibration-based structural damage identification methods. *Journal of Vibration and Shock*, **26**(10), 86–91, 2007.

[4] P.F. Rizos, N. Aspragathos and A.D. Dimarogonas, Identification of crack location and magnitude in a cantilever beam from the vibration modes, *Journal of Sound and Vibration*, **138**(3), 381–8, 1990.

[5] A. Morassi, Crack-induced changes in eigenparameters of beam structures. *Journal of Engineering Mechanics*, **119**(9), 1798–803, 1993.

[6] Y. Narkis. Identification of crack location in vibration simply supported beams. *Journal of Sound and Vibration*, **172**(4), 549–558, 1994.

[7] F. Vestroni and D. Capecchi. Damage evaluation in cracked vibrating beams using experimental frequencies and finite element models. *Journal of Vibration and Control*, **2**, 69–86, 1996.

[8] M. Chati, R. Rand and S.J. Mukherjee. Modal analysis of a cracked beam. *Journal of Sound and Vibration*, **207**, 249–70, 1997.

[9] S.M. Cheng, X.J. Wu, W. Wallace W and A.S. Swamidas. Vibrational response of a beam with breathing crack. *Journal of Sound and Vibration*, **225**(1), 201–8, 1999.

[10] P.N. Saavedra and L.A. Cuitio. Crack detection and vibration behavior of cracked beams. *Computers and Structures*, **79**(16), 1451–6, 2001.

[11] J. Fernández-Sáez and C. Navarro, Fundamental frequency of cracked beams in bending vibrations: An analytical approach. *Journal of Sound and Vibration*, **256**(1), 17–31, 2002.

[12] A. Nandi and S. Neogy. Modelling of a beam with a breathing edge crack and some observations for crack detection. *Journal of Vibration and Control*, **8**(5), 673–93, 2002.

[13] A. Chatterjee. Structural damage assessment in a cantilever beam with a breathing crack using higher order frequency response functions. *Journal of Sound and Vibration*, **329**(16), 3325–34, 2009.

[14] F.B. Sayyad and B. Kumar. Theoretical and experimental study for identification of crack in cantilever beam by measurement of natural frequencies. *Journal of Vibration and Control*, **17**(8), 1235–1240, 2011.

[15] Y.S. Jenq and S.P. Shah, A two parameter fracture model for concrete. *Journal of Engineering Mechanics*, **111**(4), 1227–1241, 1985.

[16] W.G. Halvorsen and D.L. Brown, Impulse technique for structural frequency response testing. *Sound and Vibration*, November, 8–21, 1977.

[17] J. He and Z. Fu. *Modal Analysis*. Butterworth-Heinemann, 2011.

[18] *ANSYS. Structural analysis guide – release 11.0*, ANSYS Inc., 2007.

[19] J. Domínguez, *Boundary elements in dynamics*, Computational Mechanics publications, Southampton, UK, 1993.

[20] O.C. Zienkiewicz, R.L. Taylor and J.Z. Zhu, *The finite element method: its basis and fundamentals*, Butterworth-Heinemann, 6th ed. 2005.

[21] B. Karihaloo. *Fracture Mechanics and Structural Concrete*. Longman Scientific and Technical. USA, 1995.

[22] RILEM TC89-FMT 1991. Determination of fracture parameters (KICs and CTODc) of plain concrete using three-point bend tests. *Materials and Structures*, **23**(38), 457–460, 1991.